

Synthesis and Structure of Dimeric
[(*cis*-Py₃Im)*M*]₂ Complexes [*M* = Ni, Cu, Zn;
(*cis*-Py₃Im) = *cis*-2,4,5-Tri(2-pyridyl)imidazoline]

Miguel Parra-Hake,[†] Martin L. Larter,[‡]
 Peter Gantzel,[§] Gerardo Aguirre,[†] Fernando Ortega,[†]
 Ratnasamy Somanathan,[†] and Patrick J. Walsh^{*,†,‡}

Centro de Graduados e Investigación, Instituto Tecnológico
 de Tijuana, Apartado Postal 1166,
 22000 Tijuana, B.C. Mexico,
 Department of Chemistry, San Diego State University,
 San Diego, California 92182-1030, and Department of
 Chemistry, University of California, San Diego,
 San Diego, California 92093

Received February 18, 2000

The assembly of supramolecular architectures has received significant interest due to the useful electronic, magnetic, optical, and catalytic properties of these materials.^{1,2} Synthetic routes to metal–organic coordination networks with these properties based on the self-assembly of coordinatively unsaturated metal species with nitrogen-based ligands have proven successful.^{3–11} We are interested in the design of building blocks which can be used as precursors for the synthesis of supramolecular materials. We have recently reported the synthesis and structure of a new polypyridyl ligand, *cis*-2,4,5-tri(2-pyridyl)imidazoline (*cis*-Py₃Im, **1**, eq 1).¹² Large quantities of **1** were synthesized in a single step from commercially available 2-pyridinecarboxaldehyde and ammonium hydroxide in up to 84% recrystallized yield. This remarkable reaction proceeds cleanly via an electrocyclic ring closure to give exclusively the *cis* isomer of the imidazoline.

The geometry of the ligand **1** has been determined by X-ray crystallography¹² and can be seen from the ball-and-stick drawing of **1** illustrated in Figure 1. The *cis* orientation of the 4- and 5-(2-pyridyl) groups of **1** is clear from the figure, although in the solid state the nitrogen of one of the pyridyl rings was directed away from the binding pocket defined by

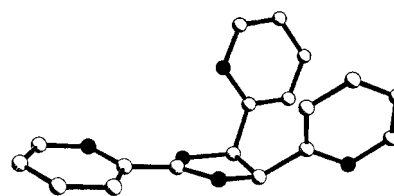
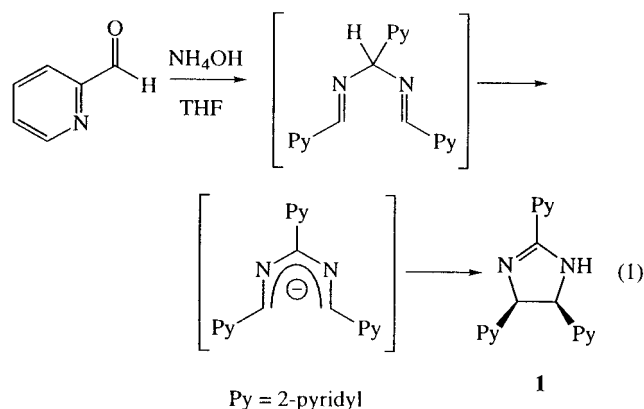


Figure 1. Ball-and-stick drawing of the structure of **1**. The black spheres represent nitrogen atoms and the white carbon atoms.



these two pyridyl groups. As suggested by the geometry of **1**, the ligand has two independent bidentate sites that are each anticipated to bind the metal in a *cis* fashion. The 2-(2-pyridyl) group and the imidazoline nitrogen comprise one binding site, and the *cis* 4- and 5-(2-pyridyl) groups form the second. Given the strong affinity of late transition metals for pyridine-based ligands,¹³ we wanted to explore the bonding and reactivity of **1** with various dicationic metals with weakly coordinating anions. Herein we describe the synthesis and structure of complexes of **1** with Ni(II), Cu(II), and Zn(II). These complexes are potentially useful monomers for the formation of linear polymers after deprotonation of the imidazoline N–H.

Results and Discussion

Synthesis of Adducts of 1. The combination of the high affinity of metals for pyridine-based ligands and the rigid framework of the bis(bidentate) ligand **1** allows for the facile preparation of complexes of **1**. Adducts of the ligand **1** are easily prepared from metal complexes with weakly coordinating counterions. The choice of solvents for the syntheses of the adducts was dependent on the solubility of the metal precursors and the ligand **1**. The ligand is soluble in organic solvents and insoluble in water. However, under acidic conditions **1** is protonated at the imidazoline nitrogen, providing a water soluble source of the ligand.

The nickel complex of **1** was prepared by combining a solution of **1** in methanol with NiSO₄·6H₂O in water (Scheme 1). Mixing of these reagents resulted in the formation of a green solution. Crystallization was induced by vapor phase diffusion of diethyl ether into the reaction mixture, which provided amber crystals of the dimer (*cis*-Py₃Im)₂Ni₂(SO₄)₂ (**2**) in 94% yield.

Synthesis of the copper derivative was performed by combining 2 equiv of **1** with 1 equiv of aqueous sulfuric acid. The protonated ligand, **1H**⁺, was soluble in water. Cu(SO₄)·5H₂O

* Author to whom correspondence should be addressed. Current address: University of Pennsylvania, 231 South 34th Street, Philadelphia, PA 19104-6323. E-mail: pwalsh@sas.upenn.edu.

[†] Centro de Graduados e Investigación, Instituto Tecnológico de Tijuana.

[‡] San Diego State University.

[§] Center for Structural Determination, University of California, San Diego.

(1) Lehn, J.-M. *Supramolecular Chemistry: Concepts and Perspectives*; VCH Publishers: New York, 1995.

(2) Desiraju, G. R. *Crystal Engineering: The Design of Organic Solids*; Elsevier: New York, 1989.

(3) Gardner, G. B.; Venkataraman, D.; Moore, J. S.; Lee, S. *Nature* **1995**, *374*, 792–795.

(4) Janiak, C. *Angew. Chem., Int. Ed. Engl.* **1997**, *36*, 1431–1434.

(5) Kahn, O.; Martinez, C. J. *Science* **1998**, *279*, 44–48.

(6) Batten, S. R.; Robson, R. *Angew. Chem., Int. Ed.* **1998**, *37*, 1460–1494.

(7) Yaghi, O. M.; Li, H.; Davis, C.; Richardson, D.; Groy, T. L. *Acc. Chem. Res.* **1998**, *31*, 474–484.

(8) Lin, W.; Evans, O. R.; Xiong, R.-G.; Wang, Z. *J. Am. Chem. Soc.* **1998**, *120*, 13272–13273.

(9) Linton, B.; Hamilton, A. D. *Chem. Rev.* **1997**, *97*, 1669–1680.

(10) Aoyagi, M.; Biradha, K.; Fujita, M. *J. Am. Chem. Soc.* **1999**, *121*, 7457–7458.

(11) Fujita, M. *Chem. Soc. Rev.* **1998**, *27*, 417–425.

(12) Larter, M. L.; Phillips, M.; Ortega, F.; Aguirre, G.; Somanathan, R.; Walsh, P. J. *Tetrahedron Lett.* **1998**, *39*, 4785–4788.

(13) Reedijk, J. In *Comprehensive Coordination Chemistry*; Wilkinson, G., Ed.; Pergamon Press: Oxford, 1987; Vol. 2, pp 73–98.

Scheme 1

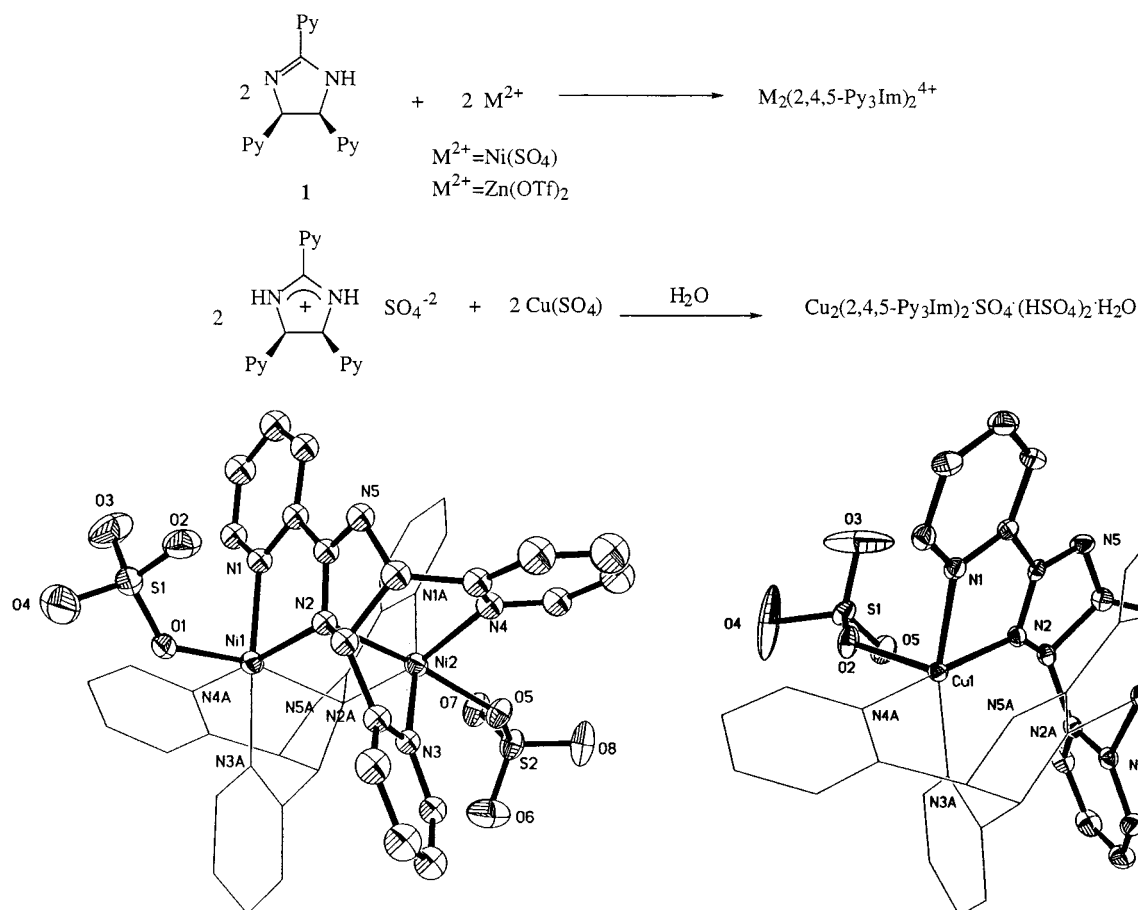


Figure 2. Structure of the dimer **2**. For clarity, one ligand is drawn in an ORTEP format while the other is illustrated as a line drawing. The second molecule in the asymmetric unit is shown in the Supporting Information. Solvent molecules are not shown.

Figure 3. Structure of the dimer **3**. For clarity, one ligand is drawn in an ORTEP format while the other is illustrated as a line drawing. Solvent molecules and nonbonded bisulfate ions are not shown.

was added as a solid, which gave a dark blue solution. Into this solution was vapor diffused acetone at room temperature. Under these conditions, large blue crystals of the mixed sulfate–bisulfate complex (*cis*-Py₃Im)₂Cu₂(SO₄)(HSO₄)₂ (**3**) formed in 91% yield. The acid–base chemistry of this reaction illustrates the change in acidity that can take place on coordination of a protonated heteroatom to a metal center. Two equivalents of the ligand was protonated with sulfuric acid to generate **1H**⁺ (Scheme 1). This indicates that bisulfate (*pK*_a = 1.99) is sufficiently acidic to protonate **1**, as expected.¹⁴ However, on coordination to copper(II), the acidity of the protonated ligand **1H**⁺ is increased such that a proton from an intermediate copper(II)–ligand adduct is able to protonate sulfate, resulting in the formation of 2 equiv of bisulfate.

The zinc analogue **4** was prepared by adding Zn(OSO₂CF₃)₂ to an acetonitrile solution of **1** (Scheme 1). Gas phase diffusion of diethyl ether into the resulting clear solution provided colorless crystals of (*cis*-Py₃Im)₂Zn₂(OSO₂CF₃)₄ (**4**) in 79% yield.

Structures of 2–4. The structures of the dimers **2–4** were determined by X-ray crystallography and are illustrated in Figures 2–4. Select bond distances and bond angles are listed in Tables 1 and 2, respectively. Details of the crystal and data collection parameters are outlined in Table 3. Due to the complexity of the structures, they have been depicted showing

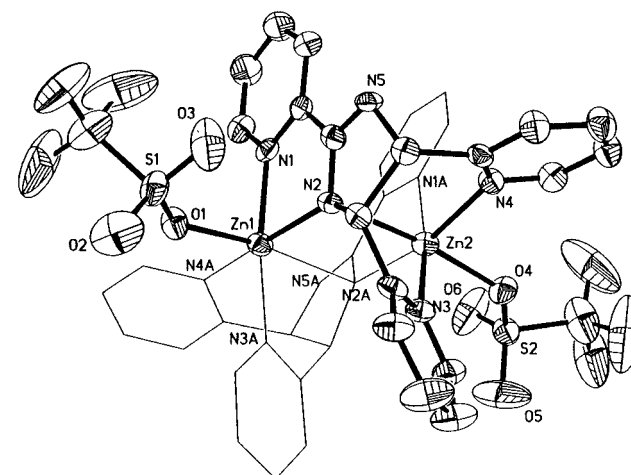


Figure 4. Structure of the dimer **4**. For clarity, one ligand is drawn in an ORTEP format while the other is illustrated as a stick structure. Solvent molecules and nonbonded triflate ions are not shown.

one of the two ligands in the normal ORTEP format while the second ligand has been illustrated as a stick structure for clarity. The structures consist of two ligands and two metals bonded to form a dimeric complex. Each metal is bonded to the 2-(2-pyridyl) group and the imidazoline nitrogen of one ligand and the *cis*-4,5-(2-pyridyl) groups of the second ligand. The metals are also bonded to the oxygen of the counteranion or a molecule of water. As described below, the gross structural features of

(14) March, J. *Advanced Organic Chemistry*, 4th ed.; Wiley and Sons: New York, 1992.

Table 1. Bond Distances for Compounds 2–4

	2, M = Ni		3, M = Cu	4, M = Zn
	molecule 1	molecule 2		
M(1)–N(1)	2.110(7)	2.099(7)	2.047(5)	2.123(5)
M(1)–N(2)	2.073(7)	2.078(7)	1.991(5)	2.097(5)
M(1)–N(2A)	2.261(7)	2.246(7)	2.788(5)	2.488(5)
M(1)–N(3A)	2.062(7)	2.056(7)	1.999(5)	2.064(5)
M(1)–N(4A)	2.129(7)	2.164(7)	2.047(5)	2.2189(5)
M(2)–N(2)	2.227(7)	2.250(7)	2.722(5)	2.477(5)
M(2)–N(3)	2.072(7)	2.065(7)	2.016(5)	2.080(5)
M(2)–N(4)	2.173(7)	2.163(7)	2.043(5)	2.195(5)
M(2)–N(1A)	2.106(7)	2.089(7)	2.059(5)	2.142(5)
M(2)–N(2A)	2.087(7)	2.078(7)	1.995(5)	2.099(2)
M(1)–O	2.048(6)	2.108(6) ^a	2.184(5)	2.095(4)
M(2)–O	2.046(6)	1.950(9)	2.244(5)	2.103(4)

^a Disordered. Details in Supporting Information.**Table 2.** Bond Angles (deg) for 2–4

	2, M = Ni		3, M = Cu	4, M = Zn
	molecule 1	molecule 2		
N(1)–M(1)–N(2)	79.1(3)	79.0(3)	81.2(2)	78.7(2)
N(1)–M(1)–N(2A)	98.4(3)	99.0(3)		94.8(2)
N(1)–M(1)–N(3A)	176.3(3)	174.5(3)	163.6(2)	170.8(2)
N(1)–M(1)–N(4A)	94.3(3)	96.0(3)	93.4(2)	95.3(2)
N(1)–M(1)–O	95.0(3)	95.3(3)	98.0(2)	94.1(2)
N(2)–M(1)–N(2A)	85.6(3)	85.7(3)		83.4(2)
N(2)–M(1)–N(3A)	98.8(3)	97.0(3)	95.1(2)	99.5(2)
N(2)–M(1)–N(4A)	170.8(3)	172.6(3)	170.8(2)	168.8(2)
N(2)–M(1)–O	93.5(3)	94.5(3)	96.1(2)	96.2(2)
N(2A)–M(1)–N(3A)	78.4(3)	76.8(3)		76.1(2)
N(2A)–M(1)–N(4A)	89.1(3)	89.7(3)		87.7(2)
N(2A)–M(1)–O	166.2(2)	165.5(2)		170.8(2)
N(3A)–M(1)–N(4A)	87.5(3)	87.6(3)	88.0(2)	84.8(2)
N(3A)–M(1)–O	88.1(3)	88.8(3)	98.3(2)	95.0(2)
N(4A)–M(1)–O	93.3(3)	91.4(3)	92.1(2)	93.7(2)
N(1A)–M(2)–N(2)	99.0(3)	96.8(3)		97.0(2)
N(1A)–M(2)–N(2A)	78.4(3)	79.1(3)	80.7(2)	78.4(2)
N(1A)–M(2)–N(3)	175.3(3)	175.0(3)	169.1(2)	172.4(2)
N(1A)–M(2)–N(4)	95.7(3)	95.6(3)	94.5(2)	94.0(2)
N(1A)–M(2)–O	92.9(3)	93.8(3) ^a	92.7(2)	94.0(2)
N(2)–M(2)–N(3)	77.9(3)	78.3(3)		75.5(2)
N(2)–M(2)–N(4)	88.8(3)	88.9(3)		88.1(2)
N(2A)–M(2)–N(3)	97.6(3)	99.2(3)	98.5(2)	98.9(2)
N(2A)–M(2)–N(4)	171.5(3)	171.9(3)	172.5(2)	167.9(2)
N(2A)–M(2)–O	98.5(3)	95.9(3) ^a	86.7(2)	98.5(2)
N(1A)–M(2)–N(2)	86.1(3)	85.6(3)		83.6(2)
N(3)–M(2)–N(4)	88.0(3)	85.6(3)	85.1(2)	87.3(2)
N(2)–M(2)–O	167.9(2)	168.6(3) ^a		169.0(2)
N(4)–M(2)–O	87.8(3)	90.6(3)	99.4(2)	91.4(2)
N(3)–M(2)–O	90.3(3)	93.8(3) ^a	98.1(2)	93.5(3)

^a Disordered. Details in Supporting Information.

2–4 are similar. However, they differ in the extent of interaction of the metal centers with an imidazoline nitrogen on an adjacent ligand.

In the structure of the nickel derivative **2**, there are two molecules in the asymmetric unit. One of these is shown in Figure 2, while the other is contained in the Supporting Information. The second dimer in the structure has a minor disorder in the position of one sulfate oxygen bonded to the nickel(II) center. This disorder does not affect the dimeric core of the molecule. The bond distances and bond angles for both molecules of **2** are listed in Tables 1 and 2, respectively. The Ni centers are in distorted octahedral environments defined by three pyridyl nitrogens, an imidazoline nitrogen, a bridging imidazoline nitrogen, and the oxygen of the sulfate counterion (Figure 2). The pyridyl N–Ni distances range from 2.056(7) to 2.173(7) Å. The nonbridging imidazoline N–Ni distances also fall within this range (2.073–2.087 Å). Interestingly, to complete its octahedral coordination environment the Ni centers bridge to the imidazoline nitrogen of an adjacent ligand. The bridging

imidazoline nitrogen–Ni distances [Ni(1)–N(2A) and Ni(2)–N(2)] of 2.261–2.227 Å are longer than the imidazoline nitrogen–Ni distances [Ni(1)–N(2) and N(2)–N(2A)], which range from 2.073 to 2.087 Å. Of the structures **2**–**4**, the bridging interaction between the metal and the imidazoline nitrogens is the most intimate in the nickel complex.

The dimeric structure of the copper derivative **3** is similar to that of the Ni dimer **2**; however, there are some important differences. Unlike the octahedral nickel complex **2**, the copper complex is only five coordinate. In the case of the copper complex, there is little or no interaction between the copper and the imidazoline nitrogen on the adjacent ligand as can be seen by the Cu(1)–N(2A) distance of 2.788(5) Å and the Cu(2)–N(2) distance of 2.722(5) Å. Additionally, the Cu(1)–O(2) bond to the sulfate oxygen of 2.184(5) Å and the Cu(2)–O(1) bond of the coordinated water molecule of 2.244(5) Å are significantly longer than the Ni–O bond distances in **2** [Ni–O 2.048(6) and 2.046(6) Å]. In contrast, the Cu–N distances are shorter than the corresponding Ni–N distances. The pyridyl N–Cu bond distances range from 1.999(5) to 2.059 Å while the imidazoline N–Cu distances are 1.991(5) and 1.995(5) Å. These distances are shorter than those in the nickel and zinc complexes. The origin of the different coordination number in the copper complex and the elongated Cu–O bonds is largely due to the Jahn–Teller effect, which often manifests itself in the lengthening of two trans bonds.¹⁵

The zinc dimer **4** is similar to the copper and nickel analogues. In this structure, the zinc has a distorted octahedral geometry. The zinc metals interact with the imidazoline nitrogens on the adjacent ligand in a bridging fashion. The Zn(1)–N(2A) and Zn(2)–N(2) distances are 2.488(5) and 2.477(5) Å, respectively, which are considerably longer than the corresponding distances in the nickel dimer **2** but shorter than those found in the copper analogue **3**. The pyridyl N–Zn distances range from 2.064(5) to 2.218(5) Å. The imidazoline N–Zn distances were Zn(1)–N(2) 2.097(5) and Zn(2)–N(2A) 2.099(5) Å. The distances between zinc and the oxygen of the sulfonate, Zn(1)–O(1) and Zn(2)–O(4), were 2.095(4) and 2.013(4) Å, respectively.

In the bonding of the ligand to nickel, copper, and zinc, there are notable deviations from the idealized octahedral bond angles (Table 2). One of the most notable is the N(1)–M(1)–N(2) and N(1A)–M(2)–N(2A) angles, which fall into the range 78.4(3)–81.2(2)°. The angles in the binding pocket defined by N(3) and N(4) of the *cis*-pyridyl groups N(3)–M(2)–N(4) and N(3A)–M(1)–N(4A) are between 84.8(2)° and 88.0(3)°. Additionally, the N(1)–M(1)–N(3A) and N(1A)–M(2)–N(3) angles range from 163.6(2)° to 176.3(3)° with the angles for Cu on the low end of this range and the angles for Zn and Ni on the high side. The N(2)–M(1)–N(4A) and N(2A)–M(2)–N(4) angles are from 167.9(2)° to 172.5(2)°. These angles are constrained by the ligand geometry but do not show large differences from idealized octahedral geometries.

Conclusions. We have shown that *cis*-2,4,5-tri(2-pyridyl)-imidazoline readily forms dimeric complexes with dicationic metal complexes to give the (*cis*-Py₃Im)₂M₂⁴⁺ adducts. The geometry of the (*cis*-Py₃Im) ligand permits it to bind well with transition metals. The coordination of the imidazoline should increase the acidity of the imidazoline N–H.^{16,17} On deproto-

- (15) Cotton, F. A.; Wilkinson, G. *Advanced Inorganic Chemistry*, 5th ed.; John Wiley and Sons: New York, 1988.
- (16) Dominguez-Vera, J. M.; Camara, F.; Moreno, J. M.; Colacio, E.; Stoeckli-Evans, H. *Inorg. Chem.* **1998**, *37*, 3046–3050.
- (17) Mimura, M.; Matsuo, T.; Nakashima, T.; Matsumoto, N. *Inorg. Chem.* **1998**, *37*, 3553–3560.

Table 3. Crystallographic Data and Collection Parameters for **2–4**

	2	3	4
empirical formula	C ₇₇ H ₁₂₄ Ni ₄ N ₂₀ O ₄₃ S ₄	C ₃₆ H ₃₁ Cu ₂ N ₁₀ O ₂₁ S ₃	C ₄₄ H ₃₆ Zn ₂ N ₁₂ O ₁₂ S ₄ F ₁₂
fw	1146.27	1162.97	1411.83
space group	<i>P</i> $\bar{1}$	<i>P</i> 2 ₁ / <i>c</i>	<i>P</i> 2 ₁ / <i>n</i>
<i>a</i> , Å	15.444(7)	12.392(2)	12.208(11)
<i>b</i> , Å	15.720(11)	25.242(2)	37.67(2)
<i>c</i> , Å	23.188(11)	15.0499(12)	13.308(12)
α , deg	82.23(5)	90	90
β , deg	82.72(4)	95.930(9)	113.03(6)
γ , deg	66.96(5)	90	90
<i>V</i> , Å ³	5116(5)	4682.3(9)	5632(8)
<i>Z</i>	4	4	4
ρ_{calc} , g cm ⁻³	1.488	1.650	1.665
<i>T</i> , K	187	291	189
λ , Å	0.71073	0.71073	0.71073
μ , mm ⁻¹	0.902	1.133	1.109
<i>R</i> _w ^a %	7.69	5.93	5.41
<i>R</i> _w ^b %	18.65	15.52	11.31

$$^a R1 = \sum ||F_o| - |F_c|| / \sum |F_o|. \quad ^b wR2 = [\sum w(F_o^2 - F_c^2)^2 / \sum w(F_o^2)^2]^{1/2}.$$

nation of this N–H, the dimeric compounds of the type synthesized here should serve as ligands and permit the assembly of these units into supramolecular structures. We are currently pursuing this objective.

Experimental Section

¹H NMR spectra were obtained on a Varian Unity 500 MHz Fourier transform spectrometer at the San Diego State University NMR facility. ¹H NMR spectra were recorded relative to residual protiated solvent. ¹³C{¹H} NMR spectra were obtained at 125 MHz on the 500 MHz instruments, and chemical shifts were recorded relative to the solvent resonance. Chemical shifts are reported in units of parts per million downfield from tetramethylsilane, and all coupling constants are reported in hertz. IR spectra were obtained on a Perkin-Elmer 1600 series spectrometer. UV–vis spectra were recorded on a HP-8452A diode array spectrometer. Melting points were uncorrected. All reactions were performed under air. All reagents were purchased from Aldrich Chemical Co. and used without further purification.

[(*cis*-Py₃Im)Ni(SO₄)₂]. *cis*-2,4,5-Tripyridylimidazoline (0.095 g, 0.316 mmol) was dissolved in 3.0 mL of methanol. NiSO₄·6H₂O (0.083 g, 0.316 mmol) was dissolved in 3.0 mL of water, and the solutions were mixed at room temperature and stirred for 1 h to give a green solution. The product was crystallized by gas phase diffusion of ethyl ether into the reaction mixture at room temperature providing yellow-amber crystals, which were dried under high vacuum (0.1354 g, 0.297 mmol, 93.9%). Mp: >260 °C. IR (KBr): 3419, 3056, 2878, 1608, 1560, 1507, 1446, 1290, 1251, 1117, 1052, 1016, 798, 756, 619 cm⁻¹. UV–vis (aq 0.0107 M): λ 328 nm, ϵ = 332 L cm⁻¹ mol⁻¹, λ 360 nm, ϵ = 296 L cm⁻¹ mol⁻¹, λ 380 nm, ϵ = 291 L cm⁻¹ mol⁻¹, λ 572 nm, ϵ = 9 L cm⁻¹ mol⁻¹.

[(*cis*-Py₃Im)₂Cu₂(SO₄)(H₂O)](HSO₄)₂. *cis*-2,4,5-Tripyridylimidazoline (0.104 g, 0.345 mmol) was dissolved in 3.7 mL of aqueous H₂SO₄ (0.0052 g/mL). CuSO₄·5H₂O (0.086 g, 0.345 mmol) was added as a solid, and the mixture was stirred for 5 min at room temperature to give a deep blue solution. The product was crystallized by gas phase diffusion of acetone into the reaction mixture at room temperature, which provided dark blue crystals (0.1817 g, 0.3124 mmol, 90.6%). Mp: 137–141 °C. IR (KBr): 3386, 3051, 2889, 1606, 1560, 1465, 1116, 754, 618 cm⁻¹. UV–vis (aq 0.0101 M) λ = 334 nm, ϵ = 311 L cm⁻¹ mol⁻¹, λ = 362 nm, ϵ = 293 L cm⁻¹ mol⁻¹, λ = 380 nm, ϵ = 285 L cm⁻¹ mol⁻¹, λ = 608 nm, ϵ = 64 L cm⁻¹ mol⁻¹. Elemental analysis: Calcd for C₃₆H₃₁Cu₂N₁₀O₂₁S₃: C, 37.17; H, 2.69; N, 12.04. Found: C, 37.41; H, 2.64; N, 12.16. No resonances were observed by NMR spectroscopy.

[(*cis*-Py₃Im)Zn(MeCN)](O₃SCF₃)₂. *cis*-2,4,5-Tripyridylimidazoline (0.1363 g, 0.4528 mmol) was added as a solid to a solution of Zn(O₃SCF₃)₂ (0.077 g, 0.212 mmol) in 3.0 mL of CH₃CN, and the mixture was stirred for 5 min at room temperature to give a colorless solution. The product was crystallized by gas phase diffusion of ethyl ether into the reaction mixture at room temperature, providing colorless crystals, which were dried under high vacuum (0.251 g, 0.356 mmol, 78.5%). Mp: 295–297 °C. IR (KBr): 3368, 3242, 3080, 2900, 1608, 1560, 1466, 1440, 1260, 1171, 1033, 784, 759, 642, 579, 519 cm⁻¹. ¹H NMR (DMSO-*d*₆, 500 MHz): δ 9.71 (s, 1H), 8.9–6.7 (m, 13H), 5.88 (d, *J* = 10.4 Hz, 2H) ppm. ¹³C{¹H} NMR (DMSO-*d*₆, 125 MHz): δ 156.4, 155.1, 148.9, 148.7, 144.0, 141.7, 140.6, 135.9, 128.4, 124.5, 123.4, 122.6, 122.2, 122.0, 119.4, 116.8, 67.0, 40.4 ppm.

X-ray Crystallographic Procedures. Structures of **2 and **4**.** Crystals were isolated from the mother liquor and immediately immersed in paratone to prevent rapid loss of solvent and crystal deterioration. A crystal was selected for the X-ray diffraction study, mounted in paratone on a quartz fiber, and rapidly placed in a nitrogen gas cold stream of the cryostat of the Siemens P3/PC-diffractometer. The crystal was indexed and data collected at low temperature. Corrections for the effects of absorption anisotropy were done. Structure solutions were performed by direct methods, and structure refinement was done with the programs SHELXS and SHELXL.¹⁸ Crystallographic parameters are given in Table 3, and selected bond distances and angles are provided in Tables 1 and 2, respectively. The crystals of **3** were found to be stable with respect to solvent loss, and data was collected at room temperature on a Siemens P4-diffractometer. A procedure similar to that above was used in data collection and structure refinement.

Acknowledgment. This work was supported by Consejo Nacional de Ciencia y Tecnología (CONACYT) for Grant 25577A and CONACYT Proyecto Infraestructura (F264-E9207) for funding of an X-ray diffractometer for Instituto Tecnológico de Tijuana.

Supporting Information Available: X-ray crystallographic files in CIF format for the complexes **2–4**. This material is available free of charge via the Internet at <http://pubs.acs.org>.

IC000182Y

- (18) Sheldrick, G. M. *SHELXTL PC Version 5.03. An Integrated System for Solving, Refining and Displaying Crystal Structures from Diffractometer Data*; Siemens Analytical X-ray Instruments, Inc.: Madison, WI, 1994.